HHS Public Access

Author manuscript

Bioconjug Chem. Author manuscript; available in PMC 2016 March 09.

Published in final edited form as:

Bioconjug Chem. 2015 December 16; 26(12): 2315–2323. doi:10.1021/acs.bioconjchem.5b00568.

Dendrimer-Based Responsive MRI Contrast Agents (G1-G4) for Biosensor Imaging of Redundant Deviation in Shifts (BIRDS)

Yuegao Huang[†,‡,*], **Daniel Coman**[†,‡], **Fahmeed Hyder**[†,‡,§,*], and **Meser M. Ali**[‖,*]

Yuegao Huang: yuegao.huang@yale.edu; Fahmeed Hyder: fahmeed.hyder@yale.edu; Meser M. Ali: mali8@hfhs.org

[†]Yale University, Department of Radiology and Biomedical Imaging, New Haven, CT 06520, USA

[‡]Yale University, Quantitative Neuroscience with Magnetic Resonance (QNMR) Core Center, New Haven, CT 06520, USA

[§]Yale University, Department of Biomedical Engineering, New Haven, CT 06520, USA

[‖]Henry Ford Hospital, Department of Neurology, Detroit, MI 48202, USA

Abstract

Biosensor imaging of redundant deviation in shifts (BIRDS) is a molecular imaging platform for magnetic resonance that utilizes unique properties of low molecular weight paramagnetic monomers by detecting hyperfine-shifted nonexchangeable protons and transforming the chemical shift information to reflect its microenvironment (e.g., via temperature, pH, etc.). To optimize translational biosensing potential of BIRDS we examined if this detection scheme observed with monomers can be extended onto dendrimers, which are versatile and biocompatible macromolecules with modifiable surface for molecular imaging and drug delivery. Here we report on feasibility of paramagnetic dendrimers for BIRDS. The results show that BIRDS is resilient with paramagnetic dendrimers up to the fourth generation (i.e., G1-G4), where the model dendrimer and chelate were based on poly(amido amine) (PAMAM) and 1,4,7,10-tetraazacyclododecane-1,4,7,10-tetraacetic acid ($DOTA^{4-}$) complexed with thulium ion (Tm^{3+}). Temperature sensitivities of two prominent signals of Gn-PAMAM-$(TmDOTA^{-})_x$ (where n = 1–4, x = 6–39) were comparable to that of prominent signals in $TmDOTA^{-}$. Transverse relaxation times of the coalesced nonexchangeable protons on Gn-PAMAM-$(TmDOTA^{-})_x$ were relatively short to provide signal-to-noise ratio that was comparable to or better than that of $TmDOTA^{-}$. A fluorescent dye, rhodamine, was conjugated to a G2-PAMAM-$(TmDOTA)_{12}$ to create a dual-modality nanosized contrast agent. BIRDS properties of the dendrimer were unaltered with rhodamine conjugation. Purposely designed paramagnetic dendrimers for BIRDS in conjunction with novel macromolecular surface modification for functional ligands/drugs could potentially be used for biologically compatible theranostic sensors.

Correspondence: Y. Huang/F. Hyder, N143 TAC (MRRC), 300 Cedar Street, Yale University, New Haven, CT 06520, Tel: +1-203-785-6206; Fax: +1-203-785-6643. M. Ali, One Ford Place, 2F, Department of Neurology, Henry Ford Hospital, Detroit, MI 48202, Tel: +1- 313-874-4479; Fax: +1-313-874-4494.

The authors declare no competing financial interest.

SUPPORTING INFORMATION AVAILABLE

The Supporting Information is available free of charge on the ACS Publications website at DOI: 10.1021/acs.bioconjchem.5b00568. MALDI-TOF characterization; Water relaxation rates; Temperature and pH dependencies on NMR spectra; coefficients for temperature dependence and calculation of chemical shifts in dendrimeric chelates (PDF) This material is available free of charge via the Internet at http://pubs.acs.org.

Keywords

BIRDS; cancer; high-speed CSI; MRI; paramagnetic complex

Introduction

Tissue temperature and pH are physiological indices that are important for many medical diagnostic applications. Noninvasive magnetic resonance imaging (MRI) of temperature and pH has potential use in cancer and stroke. In clinical practice, exogenous contrast agents are used for visualization and diagnosis of tissue abnormalities.[1, 2] Typical T_1 contrast agents (e.g., Gd-DOTA$^-$) have been used to generate positive contrast in T_1-weighted images.[3] However in conventional molecular MRI with Gd^{3+}-based low molecular weight contrast agents can sometimes be difficult to use because of complications regarding specificity and quantification of the MRI contrast, primarily because these agents reflect the relaxation enhancement of the surrounding tissue water, in which the small dynamic range of intrinsic T_1 contrast can also be affected by other in vivo factors. In addition, it is challenging to detect multiple T_1 agents selectively with MRI contrast, because the effects of these multiple agents combine to cause a single measurement of T_1 relaxation change. Similarly, the selective detection of multiple T_2 agents with MRI contrast is also difficult.

As an alternative, multiple MRI contrast agents can be detected selectively through the mechanism of chemical exchange saturation transfer (CEST). For example, paramagnetic CEST agents can detect the changes in temperature, pH, and metabolites.[4–8] Another alternative method called biosensor imaging of redundant deviations in shifts (BIRDS) has also demonstrated its potential in three-dimensional molecular reporting using ultrafast chemical shift imaging (CSI) of paramagnetic complexes.[9–12] BIRDS measures the chemical shifts of nonexchangeable protons in the paramagnetic monomers, which are structurally similar to the typical T_1 contrast agents used clinically, but other lanthanide (Ln^{3+}) metal ions (e.g., Tm^{3+}, Eu^{3+}, etc.) are used in the complex instead. The Tm^{3+} ion, for example, induces large chemical shift dispersion of the protons of the molecule. The hyperfine shifts utilized in BIRDS are contributed by contact shifts (shorter distances) and pseudocontact shifts (longer distances). Paramagnetic BIRDS chelates are predominately dependent on pseudocontact shifts, but the effect of contact shifts cannot be neglected.[13] Thus, factors such as temperature and pH that induce structural variations of the chelates are manifested by the shifts. The factor of dependencies can then be characterized by CSI. BIRDS utilizes unique properties of the nonexchangeable protons, which include short T_1 and T_2 (~10^0 – 10^1 ms), insensitivity to static field inhomogeneity (i.e., T_2 is very short), lack of overlap with other resonances, and so forth.

Current BIRDS studies use low molecular weight paramagnetic monomers (e.g., Ln-DOTP^{5-}, Ln-DOTMA$^-$, Ln-DOTA-4AmP^{5-}). Despite their capability in accurate reporting of molecular readouts (e.g, temperature, pH, etc.), BIRDS studies with the low molecular weight monomers suffer from short blood half-life and wide in vivo distribution. To further improve the translational potential of BIRDS, in this study, we examined the feasibility of BIRDS with various generations of paramagnetic dendrimeric chelates. Paramagnetic

dendrimeric chelates have been studied using other MR methods (e.g, relaxation-based MRI and CEST).[14, 15] Here we sought to examine if molecular readout for BIRDS is achievable with paramagnetic dendrimers. Briefly, the molecular reporting sensitivity of newly synthesized dendrimers (up to fourth generation) was comparable to that of the parent monomer ($TmDOTA^{-}$), where the signal-to-noise (SNR) of dendrimeric BIRDS was comparable to or better than that of the monomeric BIRDS despite shortened T_2 of the coalesced nonexchangeable protons on dendrimers. We anticipate purposely designed paramagnetic dendrimeric BIRDS for a range of biomedical applications for quantitative theranostic imaging. Furthermore, conjugation of rhodamine dye with dendrimer-based BIRDS agent will make the first bimodal BIRDS agent that can be used in two different imaging modalities (i.e., MRI and optical imaging).

Results AND Discussion

We conjugated p-SCN-Bn-DOTA to the amines on the surface of PAMAM dendrimers from generation 1 (G1) to generation 4 (G4) by using isothiocyanatobenzyl group that achieved good synthesis yield (i.e., greater than 60%) and purity (Figure 1). Then, the chelation of Tm^{3+} ion for the first to fourth generations (i.e., G1 to G4) of dendrimeric conjugates was conducted successfully.

The dendrimeric complexes were characterized by MALDI-TOF mass spectra and ICP-MS. The results revealed that there were an average of 6-, 12-, 25- and 39-TmDOTA molecules conjugated with generations G1, G2, G3 and G4 dendrimers respectively (Figure S1). According to these results, the following formula were determined: G1-PAMAM-$(TmDOTA)_6$, G2-PAMAM-$(TmDOTA)_{12}$, G3-PAMAM-$(TmDOTA)_{25}$, and G4-PAMAM-$(TmDOTA)_{39}$. The attachment of rhodamine dye to the G2-PAMAM-$(TmDOTA)_{12}$ yielded a dual fluorescent and BIRDS imaging probe (i.e., Rhodamine-G2-PAMAM-$(TmDOTA)_{12}$) which can be used for both MRI and optical imaging techniques.

The NMR spectra (Figure 1) were collected using 0.69 mM G1-PAMAM-$(TmDOTA)_6$, 0.34 mM G2-PAMAM-$(TmDOTA)_{12}$, 0.30 mM Rhodamine-G2-PAMAM-$(TmDOTA)_{12}$, 0.16 mM G3-PAMAM-$(TmDOTA)_{25}$, and 0.098 mM G4-PAMAM-$(TmDOTA)_{39}$ at pH 7.4 and 35 °C and compared with $TmDOTA^{-}$. The resulting spectra showed similar paramagnetic hyperfine-shifted resonances across the four dendrimer generations, indicating consistency of the integrated structures of the dendrimers across various generations, though structural symmetry was lost when the monomers were conjugated to the dendrimers. The presence of similar chemical shift patterns across different dendrimer generations also suggested the similarity in coordination geometry of the structures.[16] Conjugation of rhodamine group with paramagnetic G2-dendrimer did not influence the chemical shifts of paramagnetic dendrimers.

Among all resonances presented in G1-G4 dendrimers, two prominent resonances (labeled P1 and P2 for simplicity) were selected for BIRDS characterization (Figure 1). These two prominent resonances likely represent coalesced nonexchangeable protons on the dendrimers. Resonances P1 and P2 were selected because they do not overlap with other lower intensity resonances, their intensities were relatively high, and they resonate on

opposite sides of the water resonance, similar to the H2 and H6 protons of $TmDOTA^{-}$. Hence, we attributed that resonances P1 and P2 in the paramagnetic dendrimers originated from the H2 and H6 protons of $TmDOTA^{-}$, respectively. With increasing generation of the dendrimer, the P1 and P2 resonances became broader. We observed the broadening of line widths for P1 from 740 Hz (for G1-dendrimer) to 2500 Hz (for G4-dendrimer). We also observed the same broadening effect of P2 resonance from 850 Hz (for G1-dendrimer) to 2670 Hz (for G4-dendrimer). We anticipated that detection of NMR spectra of dendrimers with higher generation than G4 would be difficult since much broader resonances would be expected. This can be further inferred from the relaxation studies. Relaxation times (T_1 and T_2) determined for both resonances P1 and P2 in each dendrimeric chelate showed that T_1 values (1.9 – 3.1 ms) of the resonances were similar across four generations of dendrimers, but T_2 values (0.12 – 0.43 ms) of the resonances were shorter for higher generations of dendrimers (Figure 2 and Table 1). Interestingly, conjugation of rhodamine did not affect the relaxation times of P1 and P2 protons. Furthermore, T_1 values of P1 and P2 in G2-$(TmDOTA)_{12}$ at 4T are slightly shorter than those at 11.7T, while T_2 values of P1 and P2 in G2- $(TmDOTA)_{12}$ at 4T were higher, resulting in higher T_2/T_1 ratio. This favorable feature allows translational studies with these probes at lower field strength. T_1 values of resonances in dendrimers were comparable to that of resonances in monomers, while T_2 values were about an order of magnitude smaller. T_2 shortening of the protons on the dendrimers (i.e., not the water protons per se) was anticipated because of the increasing molecular size and slower tumbling of the macromolecule in relation to the monomer. While short T_2 values can be problematic for conventional NMR detection because the SNR of a Lorentzian line decreases, the short T_2 values for the resonances in dendrimers are useable for molecular imaging because of ultra-high-speed CSI needed for BIRDS.[17] Future improvements in scanner digitizers in conjunction with pulse sequence and coil designs would further facilitate the detection of short T_2 resonances such as in the higher generation dendrimers. For example, ultrashort TE chemical shift imaging could be integrated to improve SNR in BIRDS of paramagnetic dendrimers further.[18]

The feature of increased molecular size has been taken as an advantage in designing Gd-based dendrimeric chelates for MRI contrast agents.[19, 20] The high molecular weights of dendrimer-based contrast agents have been considered to achieve higher relaxivities than low molecular weight monomeric Gd-agents.[21, 22] The water-based MRI relaxivities of dendrimeric conjugates have been shown to improve with increasing dendrimer size that causes slower rotational tumbling time, up to the G7.[23] Since the Tm^{3+} has slightly weaker electronic relaxation effect than Gd^{3+}, as expected, the water relaxivities of the Tm-dendrimers prepared in this study are smaller than those of Gd-dendrimers (Table 1). The relaxivities measured for the Tm-dendrimers (Figure S2) were in the same range as reported for other Ln-dendrimer conjugates.[24] In MRI, Ln-dendrimers have recently been developed as paramagnetic CEST agents for molecular imaging.[15, 16] In contrast to T_1 shortening of the Gd-dendrimers, the paramagnetic CEST agent sensitivities relied not only on increasing size of the dendrimers. Instead, paramagnetic CEST agent effect can be amplified by increasing the number of monomers on the amines surfaces of higher-generation PAMAM dendrimers. For example, as much as 45 μM of Eu-G5-PAMAM can be used to generate 3% CEST effect.[15] The increased r_1 relaxivities of Gd-dendrimers are more favorable at lower

magnetic field strength MRI. It is well-known that r_1 relaxivity (i.e., for water protons) typically decreases with increasing magnetic field strength.[19] The CEST method, however, would benefit at higher magnetic fields.

In this study, we have taken a different approach (i.e., BIRDS) to detect Ln-dendrimers. Unlike conventional relaxation-based MRI and diamagnetic MRS detection methods, BIRDS is a new paradigm in molecular imaging, which detects the chemical shifts of nonexchangeable protons of the paramagnetic chelates using high-speed 3D CSI. The BIRDS method with paramagnetic molecules (e.g., $TmDOTP^{5-}$ and $TmDOTMA^{-}$) has several advantages. First, the nonexchangeable protons possess extremely short relaxation times (i.e., both T_1 and T_2 are in the range of 10^{-1} to 10^{1} ms) to allow fast signal averaging. Second, the chemical shifts are shifted away from water proton resonance such that they do not overlap with other endogenous and exogenous diamagnetic signals. Moreover, the chemical shifts are highly sensitive to physiological parameters (e.g., pH and temperature, etc.) of the microenvironment to allow molecular readout. The resonances of the molecules can be used for concentration-independent molecular imaging. These unique properties of the nonexchangeable protons in paramagnetic chelates arise from the interactions between these protons and the unpaired electrons in the central paramagnetic metal ion.[25, 26] For example, methyl protons in $TmDOTMA^{-}$ have temperature sensitivity of 0.7 ppm/°C and proton resonances in $TmDOTP^{5-}$ show high pH and temperature sensitivities.[10] Moreover, dual pH and temperature sensing is possible with the same probes (i.e., Tm-DOTA-4AmP^{5-} and Yb-DOTA-4AmP^{5-}) for both BIRDS and CEST imaging.[12] We believe the high sensitivities in absolute temperature reporting can also be achieved in paramagnetic macromolecules (e.g., paramagnetic dendrimers) with BIRDS. Despite the advantages, BIRDS technique suffers from low spatial resolution voxels (e.g., ~1 μL) compared to water proton based MRI voxels (e.g., ~0.1 μL), relies on signals from exogenous agents, and requires longer acquisition windows.

BIRDS temperature characterization was performed on resonances P1 and P2 for the four generations of dendrimeric phantoms at various temperatures in the range of 25–40 °C. As the temperature increased (Figures S3–S7), proton resonances P1 and P2 shifted toward the water resonance (set to 0 ppm). Both P1 and P2 remained as single resonances upon temperature changes, indicating that these protons show similar structural changes in response to temperature variations. Although other resonances were not as outstanding as P1 and P2, they were also shifted in response to temperature changes. However, they cannot be easily utilized in BIRDS imaging. Further analysis might be required to understand the mechanism of structural response of the dendrimers to temperature changes. Temperature dependencies of chemical shifts were linear in the temperature range investigated (Figure. 3) and were fitted using

$$\delta = C_T \times T + C_0 \quad (1)$$

where δ is the chemical shift of nonexchangeable protons (i.e., P1 and P2), T is the respective temperature of the sample, C_T is the temperature sensitivity of the chemical shift and C_0 is a temperature-independent term. The coefficients C_T and C_0 were determined

from the fit of eq 1. The temperature sensitivities for P1 and P2 resonances in each dendrimer are summarized in Table 2 and the fitted coefficients for each proton resonance for the dendrimers are outlined in Table S1. The temperature sensitivities for both P1 and P2 were similar across different generations up to the third generation and decreased slightly in G4-PAMAM-$(TmDOTA)_{39}$. The lower temperature sensitivities of P1 and P2 in G4-dendrimers were probably due to less structural variation upon temperature change induced by the restricted motions because of the larger (and presumably more rigid) size. The temperature sensitivities of the proton resonances P1 and P2 were similar to the H2 and H6 proton resonances in monomeric $TmDOTA^{-}$ (i.e. −0.2 ppm/°C for H2 and 0.4 ppm/°C for H6).[27, 28] The temperature sensitivities of the proton resonances P1 and P2 in G2-PAMAM-$(TmDOTA)_{12}$ were similar to those in Rhodamine-G2-PAMAM-$(TmDOTA)_{12}$.

As presented in Table 2, the temperature sensitivities for P1 and P2 individually have opposite signs. Thus, even higher temperature sensitivities for each dendrimer can be achieved when the chemical shift differences are used for temperature determination.[12] The temperature sensitivities of the G1-G4 dendrimers are closer to the temperature sensitivity reported for the methyl protons in $TmDOTMA^{-}$, which is the most popular temperature mapping agent in vivo.[10, 29] In addition, using the chemical shift differences between P1 and P2 to determine the temperature avoids using water resonance as a chemical shift reference, which can introduce errors due to static field inhomogeneity. Temperature can be determined from the fits of temperature versus chemical shift differences (i.e., P1-P2) using the inverse equation of eq 1. The fitted coefficients are summarized in Table S2.

To investigate the pH sensitivities of the resonances in these dendrimeric chelates, five phantoms of G2-PAMAM-$(TmDOTA)_{12}$ at different pH values were prepared for BIRDS characterization. The temperature and pH dependencies of P1 and P2 in G2-PAMAM-$(TmDOTA)_{12}$ are depicted in Figure 4. Representative pH-dependent on NMR spectra are shown in Figure S8. The 3D surface plot demonstrates that P1 was insensitive to pH changes (i.e., the chemical shifts of P1 do not vary at different pH) and P2 has low sensitivity to pH changes (i.e., 0.3 ppm per pH unit). The negligible pH sensitivities of the resonances in the dendrimers were expected because no pH-sensitive functional groups or protonation sites are present in the bifunctional chelates. However, the weak pH sensitivity of P2, which could be related to proton exchange between bulk water and amine surface of the dendrimers, may be used in future for additional molecular imaging capabilities. However, more accurate imaging of pH with dendrimers for BIRDS would be possible when pH-sensitive monomers (e.g., Tm-DOTA-4AmP^{5-}) are conjugated to the amine surface of the dendrimers.

Up to the third generation, ultrafast 3D CSI acquired for both P1 and P2 demonstrates the feasibility of BIRDS with dendrimeric chelates (Figure 5). Although the T_2 for both P1 and P2 resonances in paramagnetic dendrimers were shorter than that for resonances in monomeric $TmDOTA^{-}$, their signals were resilient enough to report the temperature accurately. The corresponding temperature maps were calculated using the chemical shift differences between P1 and P2 resonances in each dendrimeric chelates. Average temperatures were 26.7 °C, 27.1 °C, and 25.6 °C for G1-PAMAM-$(TmDOTA)_6$, G2-PAMAM-$(TmDOTA)_{12}$, and G3-PAMAM-$(TmDOTA)_{25}$, respectively. Each of these samples was imaged separately and the magnet bore temperature was controlled to be

26.5±1 °C by hot air circulation. The T_2 relaxation times for the resonances in G4-PAMAM-(TmDOTA)$_{39}$ are not favorable for CSI acquisitions using the current hardware setups. However, with faster digitizers (as discussed above) 3D CSI should be possible to regain the SNR due to T_2 loss during gradient encoding and acquisitions.

An attractive feature to use dendrimers as molecular carriers considers that multiple monomers can be attached to the surface of the dendrimers; thus, one would expect that increased number of protons can be detected and possibly increased SNR could also be observed. The SNR for both P1 and P2 resonances in dendrimeric chelates were compared with H2 and H6 in the monomer (i.e., TmDOTA$^-$) because they had approximately similar chemical shift spreads. The comparisons were made for equimolar concentrations of monomeric vs dendrimeric chelates under the same experimental parameters. As shown in Figure 6, SNR was comparable for resonances between monomeric and dendrimeric chelates. All pairwise comparisons within each group were significant at the 0.05 level. While SNR increased for both monomeric and dendrimeric chelates as the concentration of each sample increased, SNR was slightly lower for resonances in G3-PAMAM-(TmDOTA)$_{25}$ and relatively higher for resonances in G1-PAMAM-(TmDOTA)$_6$ than that for resonances in monomeric TmDOTA$^-$. No large SNR enhancements were observed for equimolar dendrimeric vs monomeric chelates, primarily due to shorter T_2 for the resonances in dendrimers. Because we observed that SNR for proton resonances remained similar from 0.69 mM G1 to 0.16 mM G3 dendrimeric chelates, we postulate that shorter T_2 for resonances in G3 results in loss in SNR and more protons available for detection in G3 leads to higher SNR. The counter balance in SNR for the resonances in dendrimers suggests that SNR will be similar across different dendrimer generations. These results suggest that BIRDS with paramagnetic dendrimeric chelates (up to third generation) would offer comparable SNR as their monomeric counterparts. However, it is noteworthy that the BIRDS method is purely based on chemical shift differences; thus, the molecular sensing is independent of agent concentration. This factor may be important for BIRDS readout efficacy in situations where the dendrimer distribution is variable across tissues.

To achieve accurate temperature maps with BIRDS a minimum SNR of 10 is required. Based on this we estimate a minimum required aqueous concentration of 0.04 mM for G3-PAMAM-(TmDOTA)$_{25}$, 0.08 mM for G2-PAMAM-(TmDOTA)$_{12}$, and 0.14 mM for G1-PAMAM-(TmDOTA)$_6$. Although SNR of signals in dendrimers are comparable to that in monomers, the construct nature of dendrimers allows us to deliver much lower concentration of agents that are prone to have longer circulation time for BIRDS. Relative to the same concentration of monomers, one notes that larger concentration of Tm^{3+} could become a safety issue when the ions are found as free ions in the body. However, the Tm^{3+} ions are tightly trapped inside the molecules and therefore not toxic. Moreover, other types of biocompatible transition metal ions (i.e., Fe^{2+}) could be used to replace lanthanide metal ions.[30] In addition, the number of TmDOTA molecules attached to the dendrimer surface could be tuned to optimize the SNR in the future experiments.

Design of higher generations of paramagnetic dendrimers for BIRDS becomes difficult with current technology because of broader resonances (shorter T_2) in higher generation of dendrimers. With the model system reported in this study, comparable SNRs of resonances

allow us to deliver higher generation (i.e., up to G4) dendrimers at lower concentration. In addition, higher generation dendrimers allow attachments of variety chelates which tend to stay in the system longer allowing a larger time window for BIRDS imaging. Other advanced fast imaging techniques could be combined with BIRDS for detecting higher-generation dendrimers, such as ultrashort TE CSI.[18]

Most Monomeric paramagnetic chelates developed for BIRDS are suited for dendrimeric chelates. Molecular sensing with macromolecules would enhance the translational potentials of BIRDS, such as longer circulation time, multifunctional chelating capabilities, tunable specificity, and the ability to carry drugs. Dendrimers are popular nanostructures for surface modification with multifunctional ligands/drugs/targeting agents.[20] Thus, the paramagnetic dendrimers studied by BIRDS can possibly be further modified to include other functional groups. As an example, we showed that Rhodamine can be attached to the paramagnetic dendrimers while the BIRDS sensitivities are retained. The capability of multiligand conjugation to the surface of dendrimers allows the combination of BIRDS and other imaging modalities for the subject of interest with biocompatible probes. Furthermore, we anticipate that pH and/or metabolite sensitive probes can be attached onto the same dendrimer to allow multiparametric BIRDS detection;[12, 14] other fluorescent, PARACEST, and/or PET agents can also be attached onto the same dendrimer to allow multimodal imaging;[31, 32] nuclei acids, proteins, and/or antibodies can be attached onto the same dendrimer to enable targeting power;[33] drugs can also be attached onto the same dendrimer to form theranostic agents.[34] In addition, concerning the possible toxicity and complications, lanthanide metals could be replaced with transition metal ions for future more biologically compatible paramagnetic dendrimeric chelates[30, 35]. Current results from paramagnetic dendrimeric chelates lay a foundation for future exploration of BIRDS with macromolecules. In summary, we envision that multifunctional dendrimeric chelates can be constructed to form biocompatible targeting theranostic agents with BIRDS and thus would play valuable roles in biomedical imaging research.

Materials and Methods

All reagents used were purchased from Sigma Aldrich (St. Louis, MO) unless otherwise stated. Bifunctional chelator 2-(4-isothiocyanatobenzyl)-1,4,7,10-tetraazacyclodo-decane-1,4,7,10-tetraacetic acid (p-SCN-Bn-DOTA) was purchased from Macrocyclics (Dallas, TX). NHS-Rhodamine was obtained from Thermo Scientific (Rockford, IL). Four generations (G1-G4) of polyamido-amine (PAMAM) dendrimers solutions were purchased from Dendritech (Miland, MI). PAMAM dendrimers were first freeze-dried under vacuum and resuspended with desired buffer solutions for conjugation reactions. Dendrimeric chelates and their conjugates were purified by repeated ultrafiltration with deionized water using appropriate molecular weight cutoff Millipore's Amicon Ultra centrifugal filters. Matrix-assisted laser desorption/ionization time-of-flight (MALDI-TOF) mass spectra were acquired on an Applied Biosystems Voyager DE spectrometer at Scripps Center for mass spectrometry. The Tm(III) content was measured by inductively coupled plasma-mass spectroscopy (ICP-MS) at Chemical Solutions Ltd. ^{1}H NMR spectra were recorded on a vertical bore Bruker NMR spectrometer operating at 500 MHz. MRI and BIRDS experiments were performed on a horizontal bore 11.7 T Agilent spectrometer equipped

with custom built ^{1}H surface coil (diameter of 14 mm). The relaxation times of G2-PAMAM-$(TmDOTA)_{12}$ were also measured on a horizontal bore 4 T Bruker spectrometer equipped with custom built ^{1}H surface coil (diameter of 20 mm). All MR experiments were conducted at temperature of 35 °C, based on our previous brain temperature measurements on anesthetized rats with BIRDS.[10, 11]

Synthesis

Dendrimeric paramagnetic chelates were prepared by conjugating p-SCN-Bn-DOTA to the amine surface of the PAMAM dendrimers (1st–4th generation).

Synthesis of G1-PAMAM-$(DOTA)_6$—To synthesize G1-PAMAM-DOTA, G1-PAMAM dendrimer (12 mg, 8.4 μmol) was dissolved in sodium phosphate solution (pH 9.0) and p-SCN-Bn-DOTA (46.2 mg, 67.2 μmol) was added. The pH of the reaction was adjusted back to pH 9 by adding 1 M NaOH. Then the reaction was stirred at 40 °C for 24 h before addition of another portion of p-SCN-Bn-DOTA (46.2 mg, 67.2 μmol). The reaction was kept stirring for 48 h at pH 9. The resulting solution was subjected to repeated centrifugation against PBS and water using Amicon ultra-15 filters (3 kDa molecular weight cutoff, MWCO). The final solution was lyophilized to obtain 46.8 mg of white solid (~89% yield) and ready for metal chelation.

Synthesis of G2-PAMAM-$(DOTA)_{12}$—To synthesize of G2-PAMAM-DOTA, G2-PAMAM dendrimer (14.6 mg, 4.5 μmol) was dissolved in sodium phosphate solution (pH 9.0) and p-SCN-Bn-DOTA (49.5 mg, 72 μmol) was added. The pH of the reaction was adjusted back to pH 9 by adding 1 M NaOH. Then the reaction was stirred at 40 °C for 24 h before addition of another portion of p-SCN-Bn-DOTA (49.5 mg, 72 μmol). The reaction was kept stirring for 48 h at pH 9. The resulting solution was subjected to repeated centrifugation against PBS and water using Amicon ultra-15 filters (10 kDa molecular weight cutoff, MWCO). The final solution was lyophilized (46.1 mg of white solid obtained, ~79% yield) and ready for metal chelation.

Synthesis of G3-PAMAM-$(DOTA)_{25}$—The synthesis of G3-PAMAM-DOTA was the same as that for G2-PAMAM-DOTA. G3-PAMAM dendrimer (19.3 mg, 2.8 μmol) and p-SCN-Bn-DOTA (123.2 mg, 179.2 μmol) were used. The resulting solution was diafiltrated by using Amicon ultra-15 filters (10 kDa molecular weight cutoff, MWCO). The final solution was lyophilized and 47.6 mg of pale solid (63.6% yield) obtained and ready for metal chelation.

Synthesis of G4-PAMAM-$(DOTA)_{39}$—The synthesize of G4-PAMAM-DOTA was conducted by following the method described above for G3-PAMAM-DOTA except G4-PAMAM dendrimer (22.7 mg, 1.6 μmol) and p-SCN-Bn-DOTA (140.8 mg, 204.8 μmol) were used. The final solution was lyophilized (42.9 mg of pale yellow solid obtained, ~60.2% yield) and ready for metal chelation.

Preparation of Thulium Complexation Experiments—To synthesize paramagnetic dendrimeric chelates, for example, G1-PAMAM-$(TmDOTA)_6$, 1.2 equiv of $TmCl_3$ in H_2O

was added to a solution of G1-PAMAM-DOTA (16 mg) in H_2O (pH 6–7). The reactions were stirred at 40 °C for 48 h before EDTA was added to remove free metal ions. The final solutions were repeatedly filtered through Amicon Ultra 3 kDa MWCO filters for G1-PAMAM-$(TmDOTA)_6$. Similarly, G_x-PAMAM-$(TmDOTA)_n$ (x = 2 to 4) were also complexed with $TmCl_3$ and were purified by diafiltration using 5 kDa MWCO filter. The filtered solutions were examined by xylenol orange test to confirm no free metal ions were present. Following purification, the final dendrimeric conjugates were characterized by MALDI-TOF and ICP-MS before characterization with magnetic resonance. The average molecular weights of Tm^{3+} chelated dendrimeric conjugates were estimated to be 7263, 14814, 30961, and 51143 g/mol for G1-, G2-, G3-, and G4-dendrimers, respectively (Figure S1). The ICP results reveal that G1-, G2-, G3-, and G4-dendrimers contain an average of 6, 12, 25, and 39 chelated Tm^{3+} ions per dendrimer, respectively.

Synthesis of Rhodamine-G2-PAMAM--$(TmDOTA)_{12}$—To synthesize of Rhodamine-G2-PAMAM--$(TmDOTA)_{12}$, a solution of rhodamine-NHS (0.68 mg, 1.28 μmol) in dimethyl sulfoxide was added to a stirred solution of G2-PAMAM-$(TmDOTA)_{12}$ (9.5 mg, 0.64 μmol) in 2 mL of PBS (pH 7.5), and the reaction was stirred at room temperature for 24 h. The reaction mixture was diafiltered using Amicon Ultra centrifugal filter unit with a 10 kDa molecular weight cutoff at 4k rpm to remove hydrolytic byproducts. The solution was lyophilized to obtain 8.1 mg of solid (~0.53 μmol, ~82 % yield). The labeling degree of rhodamine was determined by measuring the absorbance of rhodamine (ε_{552} = 80000 $M^{-1}cm^{-1}$), and 1.2 molecules of rhodamine were conjugated with each dendrimer molecule.

BIRDS Characterization

Phantoms contained different concentrations of the dendrimeric chelates (i.e., 0.69 mM G1-PAMAM-$(TmDOTA)_6$, 0.34 mM G2-PAMAM-$(TmDOTA)_{12}$, 0.30 mM Rhodamine-G2-PAMAM-$(TmDOTA)_{12}$, 0.16 mM G3-PAMAM-$(TmDOTA)_{25}$, 0.098 mM G4-PAMAM-$(TmDOTA)_{39}$) in 10 mM phosphate buffer (10% D_2O) at pH 7.4 were prepared. The pH of each phantom was assessed using SevenCompact pH meter (Mettler Toledo, MA) and was adjusted with 0.1 M NaOH or 0.1 M HCl. NMR spectra were collected using pulse acquire experiments with presaturation water suppression. The spectra were line broadened (100 Hz) and first-order baseline and zero-order phase was applied. The chemical shifts of selected proton resonances were measured by fitting to a Lorentzian function. BIRDS characterization of dendrimeric chelates was assessed by measuring the chemical shifts of each resonance as a function of temperature (25 to 40 °C) for the phantoms. For G2-PAMAM-$(TmDOTA)_{12}$, phantoms at different pHs (i.e., 6.3, 6.6, 7.0, 7.4, 7.9) were prepared in the same buffer conditions as described above for BIRDS characterization. Temperature and pH sensitivities of the selected protons in G2-PAMAM-$(TmDOTA)_{12}$ were fitted to a second-order polynomial model that includes temperature, pH, and chemical shift.[12] Longitudinal (T_1) and transverse (T_2) relaxation times of selected proton resonances were measured at 35 °C with inversion-recovery and spin echo sequences, respectively, using selective pulses and short delays of 0–60 ms for T_1 and 0–0.7 ms for T_2. Single exponential functions were fitted to the data to determine T_1 and T_2 values.

Relaxivity Measurements

Phantoms of 0–0.23 mM G1-PAMAM-$(TmDOTA)_6$, 0–0.11 mM G2-PAMAM-$(TmDOTA)_{12}$, 0–0.053 mM G3-PAMAM-$(TmDOTA)_{25}$, 0–0.033 mM G4-PAMAM-$(TmDOTA)_{39}$ in PBS (pH 7.4) were prepared for relaxivity measurements. Assessments of r_1 and r_2 relaxivities using water-based relaxation (T_1 and T_2) maps were acquired on the 11.7T horizontal bore spectrometer using the ^1H RF volume coil (diameter of 40 mm). A spin-echo MRI pulse sequence was used to image a 64 × 64 slice of 4 mm thickness with 32 × 32 mm^2 field of view at 35 °C. The temperature was controlled by circulating constant-temperature hot air around the phantoms in the magnet bore and temperature was monitored by a fiber optic probe that was positioned close to the phantoms. For T_1 mapping, eight repetition times (TR) (0.3–25 s) were used, while for T_2 mapping, ten different echo time (TE) values (9 to 90 ms) were used. The T_1 and T_2 values were calculated by fitting the absolute intensities to a single exponential function.

In Vitro CSI of Dendrimeric Chelates

The phantoms (at pH 7.4) examined in BIRDS characterization were used for CSI studies. The CSI data were obtained on a 11.7 T horizontal bore spectrometer using a surface coil RF probe (14 mm) and field of view of 25 × 25 mm. CSI experiments were acquired using 17 × 17× 17 encoding steps, 512 averages and repetition time (TR) 6 ms. A 204.8 μs single-banded Shinnar-Le Roux (SLR) RF pulse was used for excitation of selected proton resonances and 2048 points were collected during acquisition. The temperature for the CSI experiments was controlled and monitored as described above. For signal-to-noise (SNR) comparison various concentrations (i.e., 0.16 mM, 0.34 mM, and 0.69 mM) of monomeric chelates (i.e., $TmDOTA^-$) were prepared using the same buffer conditions as the dendrimeric chelates. Experiments for SNR assessments of monomeric and dendrimeric chelates were performed using the same acquisition parameters as in the CSI protocol but without gradient encoding steps.

Supplementary Material

Refer to Web version on PubMed Central for supplementary material.

Acknowledgments

The authors thank colleagues at the Magnetic Resonance Research Center and Core center for Quantitative Neuroscience with Magnetic Resonance. This work was supported by grants from the National Institutes of Health (R01 CA-140102 to F.H., R01 EB-011968 to F.H., P30 NS-052519 to F.H., and K25 CA-129173-04 to M.A.).

References

1. Lanza GM, Winter PM, Caruthers SD, Morawski AM, Schmieder AH, Crowder KC, Wickline SA. Magnetic resonance molecular imaging with nanoparticles. J Nucl Cardiol. 2004; 11:733–43. [PubMed: 15592197]
2. Aime S, Castelli DD, Crich SG, Gianolio E, Terreno E. Pushing the sensitivity envelope of lanthanide-based magnetic resonance imaging (MRI) contrast agents for molecular imaging applications. Acc Chem Res. 2009; 42:822–31. [PubMed: 19534516]

3. Herborn CU, Honold E, Wolf M, Kemper J, Kinner S, Adam G, Barkhausen J. Clinical safety and diagnostic value of the gadolinium chelate gadoterate meglumine (Gd-DOTA). Invest Radiol. 2007; 42:58–62. [PubMed: 17213750]
4. Zhang S, Malloy CR, Sherry AD. MRI thermometry based on PARACEST agents. J Am Chem Soc. 2005; 127:17572–3. [PubMed: 16351064]
5. Zhang S, Trokowski R, Sherry AD. A paramagnetic CEST agent for imaging glucose by MRI. J Am Chem Soc. 2003; 125:15288–9. [PubMed: 14664562]
6. Zhang S, Wu K, Sherry AD. A Novel pH-Sensitive MRI Contrast Agent. Angew Chem Int Ed. 1999; 38:3192–3194.
7. Zhang S, Zhou K, Huang G, Takahashi M, Sherry AD, Gao J. A novel class of polymeric pH-responsive MRI CEST agents. Chem Commun (Cambridge, UK). 2013; 49:6418–20.
8. Trokowski R, Ren J, Kalman FK, Sherry AD. Selective sensing of zinc ions with a PARACEST contrast agent. Angew Chem Int Ed. 2005; 44:6920–3.
9. Coman D, Kiefer GE, Rothman DL, Sherry AD, Hyder F. A lanthanide complex with dual biosensing properties: CEST (chemical exchange saturation transfer) and BIRDS (biosensor imaging of redundant deviation in shifts) with europium DOTA-tetraglycinate. NMR Biomed. 2011; 24:1216–25. [PubMed: 22020775]
10. Coman D, Trubel HK, Hyder F. Brain temperature by Biosensor Imaging of Redundant Deviation in Shifts (BIRDS): comparison between TmDOTP5- and TmDOTMA. NMR Biomed. 2009; 23:277–85. [PubMed: 19957287]
11. Coman D, Trubel HK, Rycyna RE, Hyder F. Brain temperature and pH measured by (1)H chemical shift imaging of a thulium agent. NMR Biomed. 2009; 22:229–39. [PubMed: 19130468]
12. Huang Y, Coman D, Ali MM, Hyder F. Lanthanide ion (III) complexes of 1,4,7,10-tetraazacyclododecane-1,4,7,10-tetraaminophosphonate for dual biosensing of pH with chemical exchange saturation transfer (CEST) and biosensor imaging of redundant deviation in shifts (BIRDS). Contrast Media Mol Imaging. 2014
13. Maritim S, Huang Y, Coman D, Hyder F. Characterization of a lanthanide complex encapsulated with MRI contrast agents into liposomes for biosensor imaging of redundant deviation in shifts (BIRDS). J Biol Inorg Chem. 2014; 19:1385–98. [PubMed: 25304046]
14. Ali MM, Woods M, Caravan P, Opina AC, Spiller M, Fettinger JC, Sherry AD. Synthesis and relaxometric studies of a dendrimer-based pH-responsive MRI contrast agent. Chem –Eur J. 2008; 14:7250–8. [PubMed: 18601236]
15. Ali MM, Yoo B, Pagel MD. Tracking the relative in vivo pharmacokinetics of nanoparticles with PARACEST MRI. Mol Pharmaceutics. 2009; 6:1409–16.
16. Pikkemaat JA, Wegh RT, Lamerichs R, van de Molengraaf RA, Langereis S, Burdinski D, Raymond AY, Janssen HM, de Waal BF, Willard NP, Meijer EW, Grull H. Dendritic PARACEST contrast agents for magnetic resonance imaging. Contrast Media Mol Imaging. 2007; 2:229–39. [PubMed: 17937448]
17. Coman D, de Graaf RA, Rothman DL, Hyder F. In vivo three-dimensional molecular imaging with Biosensor Imaging of Redundant Deviation in Shifts (BIRDS) at high spatiotemporal resolution. NMR Biomed. 2013; 26:1589–95. [PubMed: 23881869]
18. Robson MD, Tyler DJ, Neubauer S. Ultrashort TE chemical shift imaging (UTE-CSI). Magn Reson Med. 2005; 53:267–74. [PubMed: 15678544]
19. Longmire MR, Ogawa M, Choyke PL, Kobayashi H. Dendrimers as high relaxivity MR contrast agents. Wiley Interdiscip Rev Nanomed Nanobiotechnol. 2014; 6:155–62. [PubMed: 24155241]
20. Tomalia DA, Reyna LA, Svenson S. Dendrimers as multi-purpose nanodevices for oncology drug delivery and diagnostic imaging. Biochem Soc Trans. 2007; 35:61–67. [PubMed: 17233602]
21. Kobayashi H, Kawamoto S, Jo SK, Bryant HL Jr, Brechbiel MW, Star RA. Macromolecular MRI contrast agents with small dendrimers: pharmacokinetic differences between sizes and cores. Bioconjugate Chem. 2003; 14:388–94.
22. Ogawa M, Regino CA, Marcelino B, Williams M, Kosaka N, Bryant LH Jr, Choyke PL, Kobayashi H. New nanosized biocompatible MR contrast agents based on lysine-dendri-graft macromolecules. Bioconjugate Chem. 2010; 21:955–60.

23. Bryant LH Jr, Brechbiel MW, Wu C, Bulte JW, Herynek V, Frank JA. Synthesis and relaxometry of high-generation (G = 5, 7, 9, and 10) PAMAM dendrimer-DOTA-gadolinium chelates. J Magn Reson Imaging. 1999; 9:348–52. [PubMed: 10077036]
24. Bulte JWM, Wu CC, Brechbiel MW, Brooks RA, Vymazal J, Holla M, Frank JA. Dysprosium-DOTA-PAMAM dendrimers as macromolecular T2 contrast agents - Preparation and relaxometry. Invest Radiol. 1998; 33:841–845. [PubMed: 9818319]
25. Reuben J. Origin of Chemical-Shifts in Lanthanide Complexes and Some Implications Thereof. J Magn Reson. 1973; 11:103–104.
26. Koehler J, Meiler J. Expanding the utility of NMR restraints with paramagnetic compounds: Background and practical aspects. Prog Nucl Magn Reson Spectrosc. 2011; 59:360–389. [PubMed: 22027343]
27. Zuo CS, Mahmood A, Sherry AD. TmDOTA-: a sensitive probe for MR thermometry in vivo. J Magn Reson. 2001; 151:101–6. [PubMed: 11444943]
28. Hekmatyar SK, Poptani H, Babsky A, Leeper DB, Bansal N. Non-invasive magnetic resonance thermometry using thulium-1,4,7,10-tetraazacyclododecane-1,4,7,10-tetraacetate (TmDOTA(−)). Int J Hyperthermia. 2002; 18:165–79. [PubMed: 12028635]
29. Hekmatyar SK, Hopewell P, Pakin SK, Babsky A, Bansal N. Noninvasive MR thermometry using paramagnetic lanthanide complexes of 1,4,7,10-tetraazacyclodoecane-alpha,alpha′,alpha″,alpha‴-tetramethyl-1,4,7,10- tetraacetic acid (DOTMA4-). Magn Reson Med. 2005; 53:294–303. [PubMed: 15678553]
30. Dorazio SJ, Olatunde AO, Tsitovich PB, Morrow JR. Comparison of divalent transition metal ion paraCEST MRI contrast agents. J Biol Inorg Chem. 2014; 19:191–205. [PubMed: 24253281]
31. Ali MM, Bhuiyan MP, Janic B, Varma NR, Mikkelsen T, Ewing JR, Knight RA, Pagel MD, Arbab AS. A nano-sized PARACEST-fluorescence imaging contrast agent facilitates and validates in vivo CEST MRI detection of glioma. Nanomedicine (London, UK). 2012; 7:1827–37.
32. Talanov VS, Regino CA, Kobayashi H, Bernardo M, Choyke PL, Brechbiel MW. Dendrimer-based nanoprobe for dual modality magnetic resonance and fluorescence imaging. Nano Lett. 2006; 6:1459–63. [PubMed: 16834429]
33. Ye M, Qian Y, Tang J, Hu H, Sui M, Shen Y. Targeted biodegradable dendritic MRI contrast agent for enhanced tumor imaging. J Controlled Release. 2013; 169:239–45.
34. Liu Y, Zhang N. Gadolinium loaded nanoparticles in theranostic magnetic resonance imaging. Biomaterials. 2012; 33:5363–75. [PubMed: 22521487]
35. Zhu J, Gale EM, Atanasova I, Rietz TA, Caravan P. Hexameric Mn(II) dendrimer as MRI contrast agent. Chem –Eur J. 2014; 20:14507–13. [PubMed: 25224391]

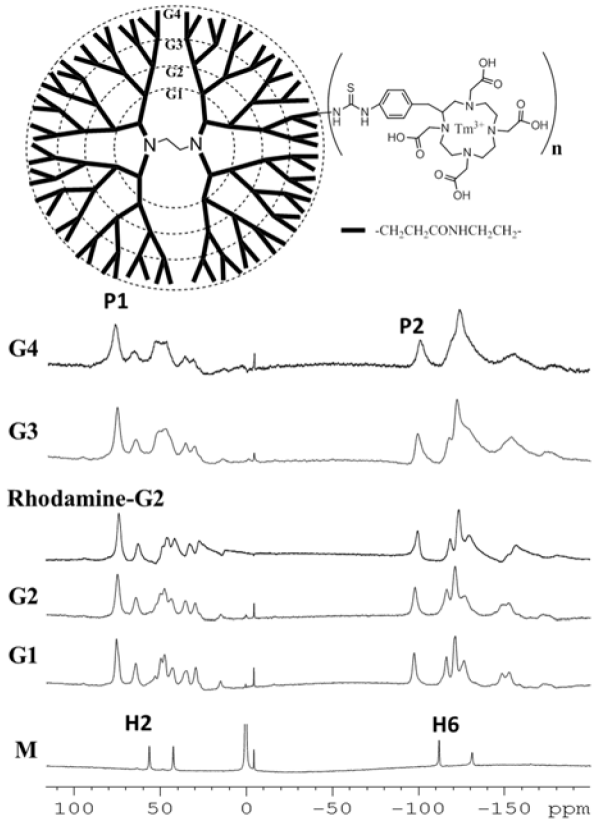

Figure 1.

Top panel: Structural illustration of dendrimeric molecules for BIRDS. Paramagnetic bifunctional chelates (isothiocyanate linked $TmDOTA^{-}$) were conjugated onto the primary amines of PAMAM dendrimers (up to 4^{th} generation). Bottom panel: NMR spectra of (M) Monomer (i.e. $TmDOTA^{-}$), (G1) G1-PAMAM-$(TmDOTA^{-})_{6}$, (G2) G2-PAMAM-$(TmDOTA^{-})_{12}$, (Rhodamine-G2) Rhodamine-G2-PAMAM-$(TmDOTA)_{12}$, (G3) G3-PAMAM-$(TmDOTA^{-})_{25}$, (G4) G4-PAMAM-$(TmDOTA^{-})_{39}$ at 35 °C and pH 7.4.

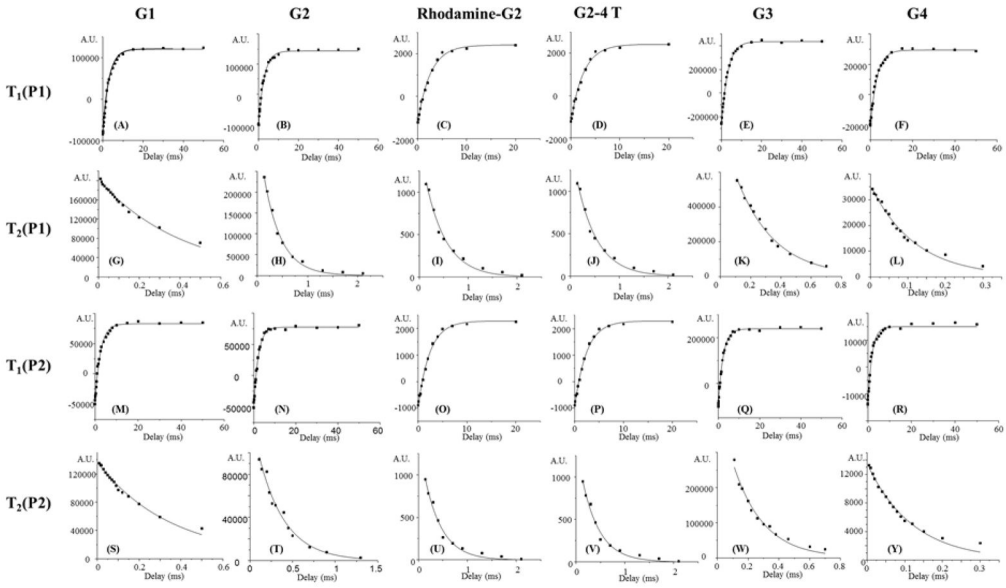

Figure 2.

Determination of ^{1}H relaxation times for resonances P1 and P2 in paramagnetic dendrimeric chelates. Longitudinal (T_1, A–F) and transverse (T_2, G–L) relaxation times at 11.7 T for P1 of (A and G) G1-$(TmDOTA)_6$, (B and H) G2-$(TmDOTA)_{12}$, (C and I) G2-$(TmDOTA)_{12}$-Rhodamine, (D and J) G2-$(TmDOTA)_{12}$ at 4 T, (E and K) G3-$(TmDOTA)_{25}$, and (F and L) G4-$(TmDOTA)_{39}$; Longitudinal (T_1, M–R) and transverse (T_2, S–X) relaxation times at 11.7 T for P2 of (M and S) G1-$(TmDOTA)_6$, (N and T) G2-$(TmDOTA)_{12}$, (O and U) G2-$(TmDOTA)_{12}$-Rhodamine, (P and V) G2-$(TmDOTA)_{12}$ at 4 T, (Q and W) G3-$(TmDOTA)_{25}$, and (R and X) G4-$(TmDOTA)_{39}$. The relaxation times are summarized in Table 1.

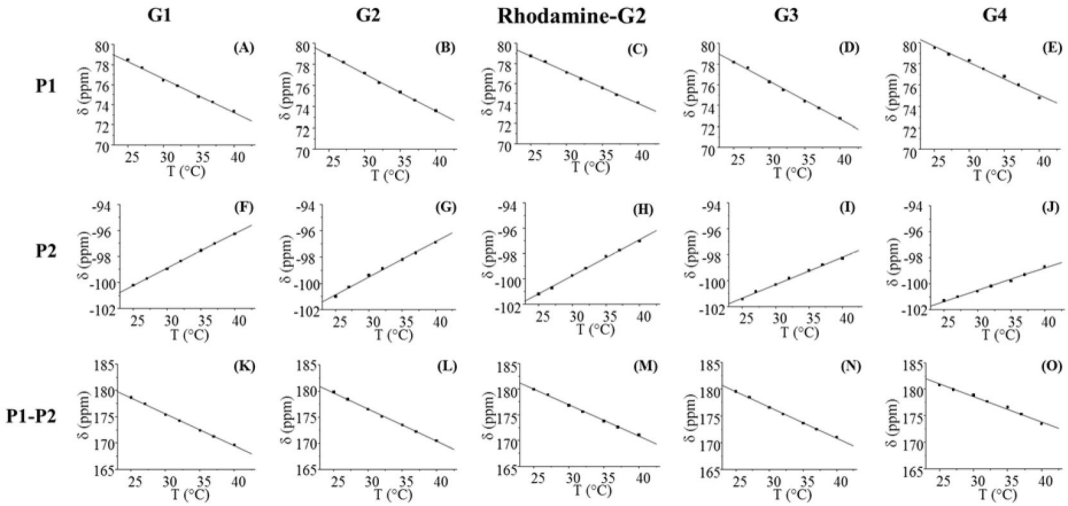

Figure 3.

BIRDS characterization. Temperature dependencies of chemical shifts of P1 and P2 and their chemical shift differences (P1-P2) in dendrimeric chelates: (A) P1, (F) P2, and (K) P1-P2 of G1-$(TmDOTA)_6$; (B) P1, (G) P2, and (L) P1-P2 of G2-$(TmDOTA)_{12}$; (C) P1, (H) P2, and (M) P1-P2 of Rhodamine-G2-$(TmDOTA)_{12}$; (D) P1, (I) P2, and (N) P1-P2 of G3-$(TmDOTA)_{25}$; and (E) P1, (J) P2, and (O) P1-P2 of G4-$(TmDOTA)_{39}$. The temperature sensitivities (C_T) of each proton determined with eq 1 are shown in Table 2.

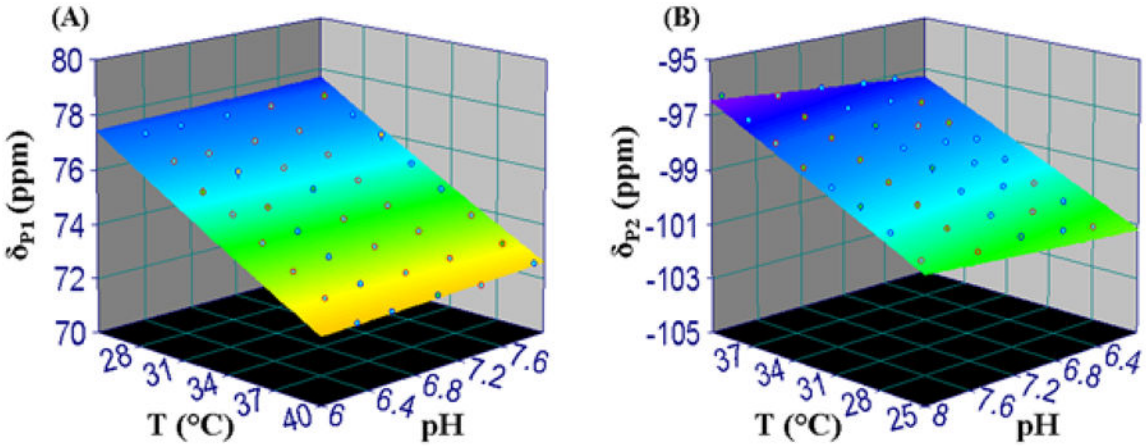

Figure 4.

Temperature and pH dependencies of (A) P1 and (B) P2 proton chemical shifts of G2-PAMAM-$(TmDOTA)_{12}$ are shown. The 3D surfaces represent the result of the fits of chemical shift, δ, as a function of temperature, T, and pH.

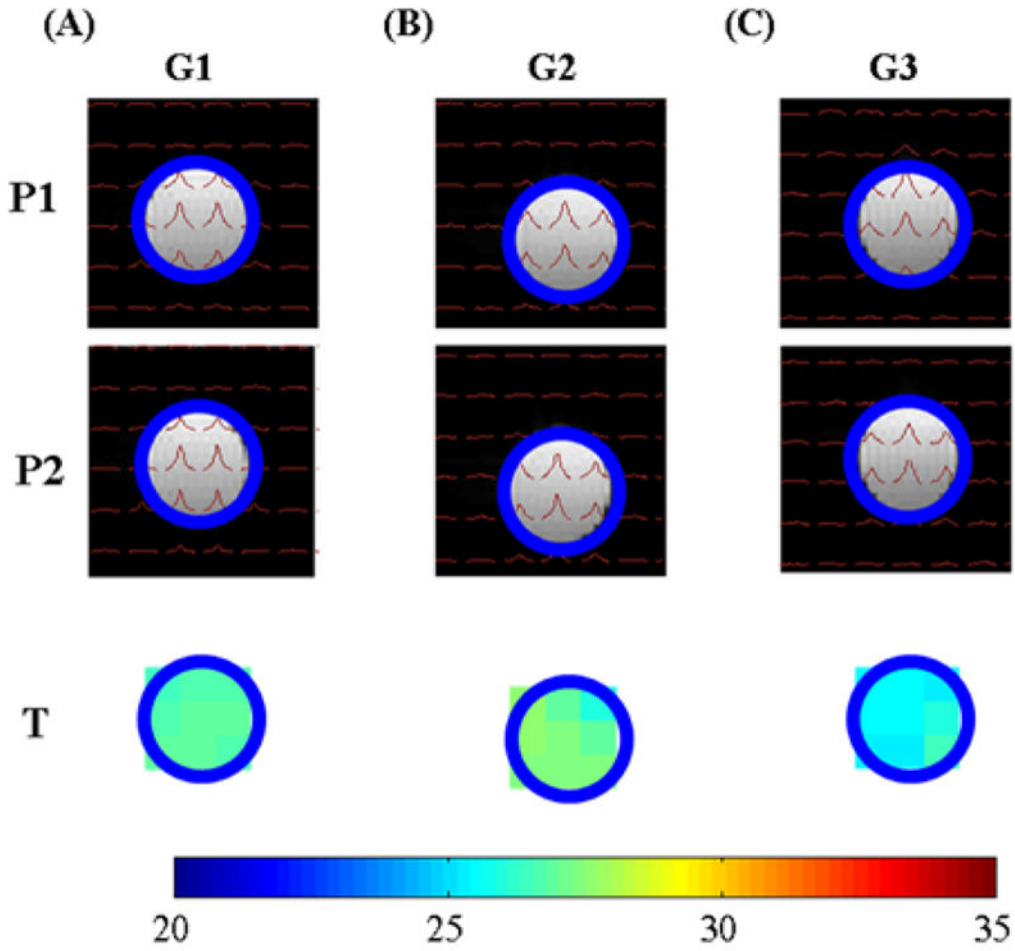

Figure 5.

3D CSI BIRDS for resonances P1 (first row) and P2 (second row) in phantoms containing (A) G1-PAMAM-$(TmDOTA)_6$, (B) G2-PAMAM-$(TmDOTA)_{12}$, and (C) G3-PAMAM-$(TmDOTA)_{25}$. The corresponding temperature maps (third row) calculated from the chemical shift difference between P1 and P2 provided temperature values of 26.7 °C, 27.1 °C, and 25.6 °C for G1-PAMAM-$(TmDOTA)_6$, G2-PAMAM-$(TmDOTA)_{12}$, and G3-PAMAM-$(TmDOTA)_{25}$, respectively.

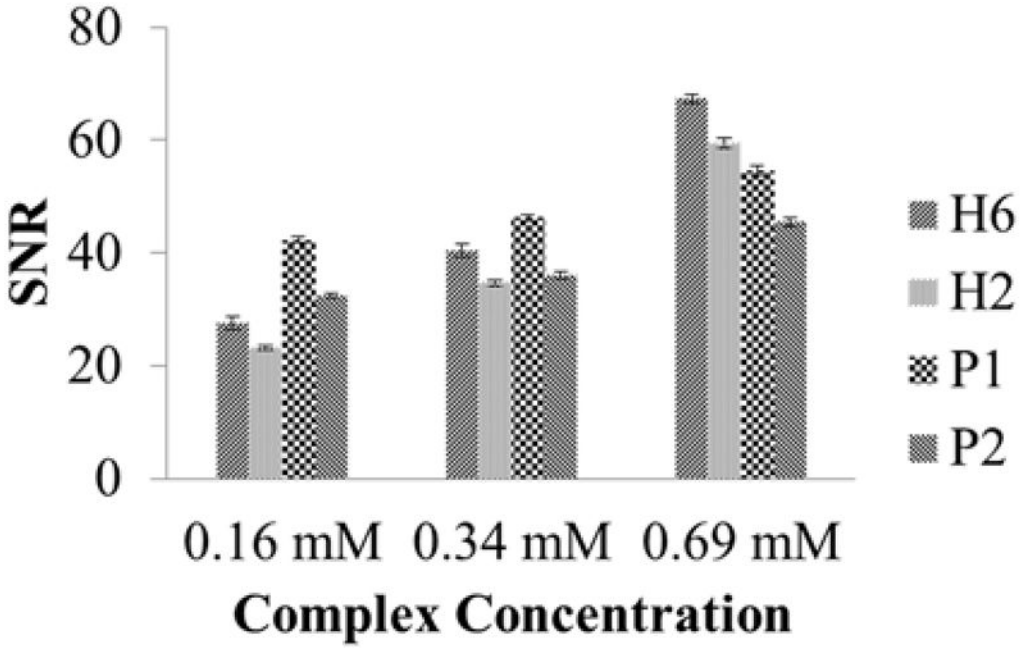

Figure 6.

SNR determination for resonances P1and P2 in dendrimeric chelates, and H6 and H2 in $TmDOTA^{-}$. The comparisons were made between the equimolar concentration of dendrimeric chelates and monomers (i.e., 0.69 mM G1-PAMAM-$(TmDOTA)_6$ vs 0.69 mM $TmDOTA^{-}$, 0.34 mM G2-PAMAM-$(TmDOTA)_{12}$ vs 0.34 mM $TmDOTA^{-}$, and 0.16 mM G3-PAMAM-$(TmDOTA)_{25}$ vs 0.16 mM $TmDOTA^{-}$).

Table 1

Water Proton Relaxivity and Relaxation Times of Proton Resonances in Dendrimeric Chelates at 35 °C

				P1		P2	
paramagnetic Chelates	**field strength (T)**	**r_1 ($s^{-1}mM^{-1}$)**	**r_2 ($s^{-1}mM^{-1}$)**	**T_1 (ms)**	**T_2 (ms)**	**T_1 (ms)**	**T_2 (ms)**
G1-$(TmDOTA)_6$	11.7	0.21 ± 0.02	1.0 ± 0.1	3.1 ± 0.1	0.43 ± 0.01	2.5 ± 0.1	0.36 ± 0.01
G2 -$(TmDOTA)_{12}$	11.7	0.22 ± 0.02	1.5 ± 0.1	2.7 ± 0.1	0.34 ± 0.02	2.1 ± 0.1	0.31 ± 0.02
G2 -$(TmDOTA)_{12}$	4	-	-	2.6 ± 0.1	0.42 ± 0.02	2.0 ± 0.1	0.36 ± 0.02
Rhodamine-G2-$(TmDOTA)_{12}$	11.7	-	-	2.8 ± 0.1	0.33 ± 0.02	2.4 ± 0.1	0.32 ± 0.02
G3 -$(TmDOTA)_{25}$	11.7	0.26 ± 0.03	1.8 ± 0.2	2.7 ± 0.1	0.25 ± 0.01	2.3 ± 0.1	0.20 ± 0.02
G4 -$(TmDOTA)_{39}$	11.7	0.27 ± 0.03	2.1 ± 0.2	3.0 ± 0.1	0.12 ± 0.01	1.9 ± 0.1	0.12 ± 0.01

Table 2

Temperature Sensitivities of Resonances in Dendrimeric Chelates

	temperature sensitivity (C_T) (ppm/°C)		
paramagnetic chelates	**P1**	**P2**	**P1-P2**
G1 -$(TmDOTA)_6$	−0.34 ± 0.02	0.27 ± 0.01	−0.61 ± 0.02
G2 -$(TmDOTA)_{12}$	−0.35 ± 0.01	0.27 ± 0.01	−0.62 ± 0.01
Rhodamine- G2 -$(TmDOTA)_{12}$	−0.33 ± 0.01	0.28 ± 0.01	−0.61 ± 0.01
G3 -$(TmDOTA)_{25}$	−0.37 ± 0.01	0.21 ± 0.01	−0.58 ± 0.01
G4 -$(TmDOTA)_{39}$	−0.31 ± 0.01	0.17 ± 0.01	−0.48 ± 0.01

Note: At 11.7T and temperature range is 25 to 40 °C.